Journal of Photochemistry and Photobiology A: Chemistry 213 (2010) 123–128

Contents lists available at ScienceDirect

Journal of Photochemistry and Photobiology A: Chemistry

journal homepage: www.elsevier.com/locate/jphotochem

An investigation of porous structure in molecularly imprinted polymer for sensor development: Non-linear fluorescence quenching of 17β-estradiol bound inside MIP submicron particles by sodium nitrite and methacrylamide

Yu Yang, Edward P.C. Lai*

Department of Chemistry, Ottawa-Carleton Chemistry Institute, Carleton University, 1125 Colonel By Drive, Ottawa, Ontario K1S 5B6, Canada

ARTICLE INFO

Article history:
Received 1 March 2010
Received in revised form 12 May 2010
Accepted 16 May 2010
Available online 9 June 2010

Keywords:
Poly(MAA-co-EGDMA)
MIP submicron particles
17β-Estradiol
Fluorescence quenching
Porous structure

ABSTRACT

17β-Estradiol (E2) molecularly imprinted and non-imprinted poly(methacrylic acid-co-ethylene glycol dimethacrylate) submicron particles (MIP and NIP) have been synthesized in the presence and absence of template E2 molecules. The sizes of MIP and NIP particles were determined via a nanoDLS particle size analyzer to be 477 ± 11 and 373 ± 21 nm. After these naturally non-fluorescent MIP and NIP particles bound with E2 molecules as a fluorophore, strong fluorescence at λ_{em} = 310 ± 1 nm was detectable when excited by light of λ_{ex} = 280 ± 1 nm. Sodium nitrite and methacrylamide were selected as two fluorescence quenchers with different ionic/molecular sizes. They both exhibited non-linear quenching behavior in the Stern–Volmer plots. The smaller quencher (sodium nitrite) ionized in water to produce nitrite anions that easily penetrated into the porous MIP particles and quenched the fluorescence emission from the E2 molecules bound inside. It produced a dynamic quenching constant (K_{sv}) of 23.0 ± 1.3 M^{-1} when the concentration of E2–MIP particles was 2.5 mg/mL in water. The larger quencher (methacrylamide) was sterically hindered in penetrating the pores of MIP particles. Its dynamic quenching constant (K_{sv}) hence became small, to be less than 1.0 ± 0.5 M^{-1}. This approach enabled an investigation of the porous structure in MIP particles for development of a novel E2 sensing scheme.

1. Introduction

MIP is increasingly recognized as a selective separation material ever since 1990s the growth in the number of published articles [1]. Every MIP consists of a highly cross-linked polymer matrix and one target compound as the template. After the template is eluted, binding cavities become available in the MIP with high affinity for the target compound as analyte. The advantages of MIP technology are high selectivity for the analyte, and hence low detection limits due to less matrix interference effects. MIPs can be used in sample solutions over a broad pH or temperature range. They can also be prepared at both high cost- and time-efficiencies. Nowadays MIPs are broadly benefiting the senor and separation technologies. They are commonly used in thermometric sensors for amino acids and carbohydrates [2], optical sensors for biologically active molecules [3], ionic sensor [4], biomimetic electrochemical sensors [5], enantiomer separations [6] and solid phase extractions [7].

Estrogens are naturally produced female sex steroid hormones. They were first described by Stockard and Papanicolaou [8]. Then, Allen and Doisy isolated estrogens and tested the estrogenic activities in 1923 [9]. As shown in Fig. 1, estrone (E1) is the primary estrogenic hormone in the post-menopausal woman. β-Estradiol (E2) is the primary estrogen of ovarian origin and the major estrogenic hormone in the pre-menopausal woman. E2 has a relative strength that is 12 times greater than E1 and 80 times higher than estriol (E3). E3 is a relatively weak estrogen which yields from the metabolism of estrone; it reaches the highest level in women only during pregnancy.

Estrogens can cause major impact on reproduction, sex characteristics and regulation of female development, and infertility [10–15]. Moreover, estrogens are carcinogenic compounds especially toward women breast and endometrial cancers.

One sensing method for determination of the most naturally abundant estrogen E2 in water by spectrofluorimetry is undergoing rapid development in our laboratory. It involves (a) addition of MIP particles to bind E2 in a water sample, (b) modification of the water sample to release non-specifically bound E2 (and other compounds) from MIP particles, (c) quenching of fluorescence emission from E2 (and other compounds) in the water by methacrylamide, (d) preconcentration of MIP particles into a small cell volume, (e) measurement of fluorescence emission intensity from E2 specif-

* Corresponding author. Tel.: +1 613 520 2600x3835; fax: +1 613 520 3749.
E-mail address: edward_lai@carleton.ca (E.P.C. Lai).

1010-6030/$ – see front matter © 2010 Elsevier B.V. All rights reserved.
doi:10.1016/j.jphotochem.2010.05.010

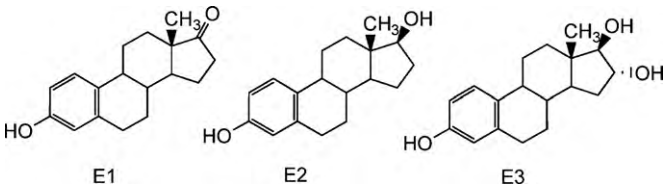

Fig. 1. Molecular structures of estrone (E1), β-estradiol (E2) and estriol (E3).

ically bound inside MIP particles, (f) quenching of fluorescence emission from E2 inside MIP particles by sodium nitrite and (g) blank measurement of fluorescence emission intensity from MIP particles. After subtracting (g) from (f), the concentration of E2 can be determined from a standard calibration curve. This E2 concentration will be divided by the preconcentration factor to obtain a final result.

The objective of this work was to investigate the porous structure of MIP particles for non-linear fluorescence quenching of E2 (bound inside them) by sodium nitrite and methacrylamide. Our goal was to determine whether any larger quenchers would be needed to fulfill step (c) in the method described above.

2. Experimental

2.1. Chemicals

17β-Estradiol (E2) and sodium nitrite were purchased from Sigma–Aldrich (St. Louis, MO, USA). Methacrylic acid and methacrylamide were purchased from Aldrich (Milwaukee, WI, USA). 2,2-Azobisisobutyronitrile (AIBN) was purchased from Pfaltz & Bauer (Waterbury, CT, USA). HPLC grade methanol, HPLC grade acetonitrile and Spectro grade acetone were purchased from Caledon (Georgetown, ON, Canada). 18 MΩ cm distilled deionized water (DDW) was obtained from a Millipore Milli-Q water system (Bedford, MD, USA).

2.2. Preparation of E2–MIP and NIP submicron particles

The method for preparation of E2-molecularly imprinted polymer (E2–MIP) and non-imprinted polymer (NIP) submicron particles had previously been described [16]. The freshly prepared MIP and NIP particles in suspension were separately placed in five 15 mL polypropylene tubes (Greiner Bio-One, Frickenhausen, Germany) and then spun by a centrifuge (Hamilton Bell VanGuard Centrifuge, Montvale, NJ, USA) for 60 min at 4000 rpm to help remove the supernatants.

2.2.1. MIP particles

The E2–MIP particles were washed in 15 mL of DDW with ultrasonication (Branson 2510, Danbury, CT, USA) for 30 min to remove free E2 and pre-polymerization residues. After more than 25 times of washing, the pH was 5.5 ± 0.1 in the supernatant and the free E2 concentration was lower than 0.2 ppm (the detection limit of our HPLC-FD instrument).

2.2.2. NIP particles

The NIPs particles were washed by methanol, acetonitrile and DDW, three times each, to obtain a final pH of 5.5 ± 0.1 in the supernatant. 50 mg of NIP particles were then suspended in 15 mL of 3.5 ppm E2 aqueous solution. The suspension was sonicated for 1 h, allowing binding between the NIP particles and E2 to form E2–NIP particles.

2.3. Characterization of particles

2.3.1. Particle size measurements by dynamic light scattering (DLS)

The washed MIP and NIP particles were suspended in 10 M KNO_3 at a concentration of 40 μg/mL. The suspensions were sonicated for 15 min before measurement on a NanoDLS particle size analyzer (Brookhaven Instruments, Holtsville, NY, USA). The instrument had been calibrated by 92 ± 4 nm Nanosphere™ size standards (Duke Scientific, Palo Alto, CA, USA). A total of 10 measurements were run after 30 s, and the laser beam intensity was automatically optimized by the instrument before each run.

2.3.2. Fluorescence binding measurements

2.3.2.1. MIP particles. Fluorescence emission of the last washing from Section 2.2.1 was measured by a fluorescence spectrophotometer (Varian Cary Eclipse, Palo Alto, CA, USA) using excitation wavelength of 279 ± 1 nm and emission wavelength of 310 ± 1 nm (or scanning from 290 to 450 nm). Both the excitation and emission slits were set at 5 nm. Fluorescence emission of the washed E2–MIP particles suspension was measured using the same spectrophotometer settings. All fluorescence experiments were carried out at room temperature (20 ± 1 °C).

2.3.2.2. NIP particles. Fluorescence emissions of the 3.5 ppm E2 aqueous solution and the supernatant after binding from Section 2.2.2 were measured using the same spectrophotometer settings as in Section 2.3.2.1.

2.3.3. Fluorescence quenching measurements

Fluorescence emission spectra of 0.5–4.5 ppm E2 aqueous solutions and 0.1–2.5 mg/mL E2–MIP and E2–NIP particles, suspended in DDW, were measured using the same spectrophotometer settings as in Section 2.3.2. All these fluorescence measurements were carried out in a 3 mL quartz cuvette cell with a PTFE stopper. Next, these E2 solutions and E2–MIP and E2–NIP particle suspensions were successively spiked with 1 mg of quencher (sodium nitrite or methacrylamide) before the fluorescence emission spectra were measured again. The inner filter effect for right-angle illumination, introduced by the absorption of exciting light (λ_{ex} = 280 ± 1 nm) and absorption of fluorescence emission (λ_{em} = 310 ± 1 nm) by quenchers, were corrected as described elsewhere [17]. All light absorptions by quenchers were measured on a UV–visible spectrophotometer (Varian Cary 3, Palo Alto, CA, USA) by scanning from 250 to 350 nm at room temperature (20 ± 1 °C).

3. Results and discussion

3.1. Fluorescence property of E2–MIP and E2–NIP particles

The spherical MIP particles were determined by DLS to have an average diameter of 477 ± 11 nm. The spherical NIP particles were smaller, with an average diameter of 373 ± 21 nm. According to the general theory of molecular imprinting, MIP bound E2 via specific, semi-specific and non-specific interactions, whereas NIP bound E2 via non-specific interaction only [18]. Both MIP and NIP particles prepared with MAA and EGDMA were not naturally fluorescent. However, once the MIP and NIP particles bound some E2 molecules, the bound E2 was detectable by a fluorescence spectrophotometer. Fig. 2(a) and (b) shows the fluorescence emission peak at 310 ± 1 nm from E2–MIP to E2–NIP particles, respectively when using an excitation wavelength of 280 ± 1 nm. Note that the emission spectra from E2–MIP to E2–NIP particles were very similar to that obtained from 3.5 ppm E2 in aqueous solution (Fig. 2c) except for two light scattering peaks at 380 ± 1 and 423 ± 1 nm from the particles.

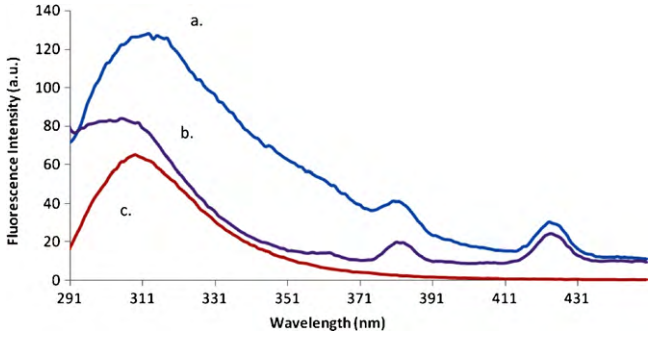

Fig. 2. Fluorescence determination of E2 binding with MIP and NIP particles (λ_{ex} = 280 ± 1 nm): (a) fluorescence emission of E2–MIP particles suspended in DDW, (b) fluorescence emission of E2–NIP particles suspended in DDW and (c) fluorescence emission of 3.5 ppm E2 in aqueous solution.

The detection sensitivity for E2–MIP/NIP fluorescence was not significantly decreased by the physical and chemical properties of particles. The fluorescence emission intensity of 3.5 ppm E2 was 65 ± 1 a.u. before binding with NIP particles. After binding with 50 mg of NIP particles the fluorescence emission intensity in the same solution (supernatant) decreased to 5 ± 1 a.u. Apparently 92 ± 1% of E2 (48.4 ± 0.1 μg) in the original aqueous solution was bound by NIP particles.

3.2. Fluorescence quenching analysis

Fluorescence quenching of the E2 molecules bound inside MIP and NIP particles is significant to study for clarifying the binding site environment between E2 and MIP/NIP. The results, as detailed below, will show some essential differences between MIP and NIP when they bound with E2 molecules.

The process of fluorescence quenching is described by the Stern–Volmer equation:

$$\frac{F_0}{F} = 1 + K_{SV}[Q] \quad (1)$$

where F_0 and F are the fluorescence emission intensities from E2 detected in the absence and presence of a quencher, respectively. K_{sv} is Stern–Volmer florescence quenching constant (dynamic or collisional quenching constant) and [Q] is the concentration of quencher. Sodium nitrite and methacrylamide were selected for comparison of their quenching properties [3,4]. These two quenchers represent different types of chemical species. One is an ionic quencher; sodium nitrite exists in aqueous solution in the form of (positively charged sodium ions and) negatively charged nitrite ions. This nitrite anion interacted with E2 to result in fluorescence quenching. The other one is a molecular quencher; methacrylamide with specific functional groups (acryl and amide) has good water solubility for fluorescence quenching. No attempt was made in this study to analyze these two factors (size and ionic charge) separately.

Fig. 3(a) shows the fluorescence emission spectra of 4.5 ppm E2 aqueous solution progressively quenched by titration with sodium nitrite. The concentration of sodium nitrite titrated into 3 mL of 4.5 ppm E2 aqueous solution increased from 0.00 to 0.19 M, with each titration increment amounting to 1 mg (10 μL of 100 ppm) of sodium nitrate. The fluorescence emission intensity was obviously decreased, after 45 titration increments, by 99% from the initial intensity. During the quenching titration, the fluorescence peak shape changed from sharp to broad. Fig. 3(b) and (c) shows how progressively the fluorescence emissions of 2.5 mg/mL E2–MIP and E2–NIP particles in aqueous suspensions were quenched by titration with sodium nitrite. The lower fluorescence intensity scale in

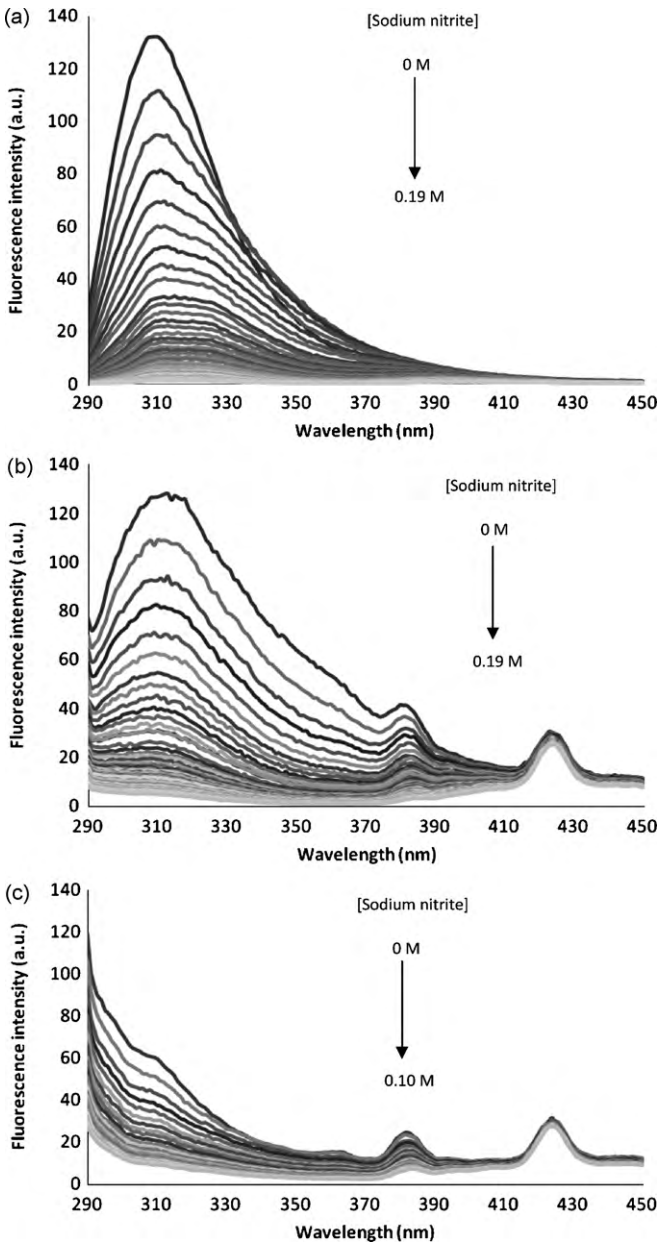

Fig. 3. Fluorescence emission spectra of (a) 4.5 ppm E2 aqueous solution, (b) 2.5 mg/mL E2–MIP particles in aqueous suspension and (c) 2.5 mg/mL E2–NIP particles in aqueous suspension, during titration with sodium nitrite up to a final concentration of 0.19 M (without causing any significant dilution effects, ~6%).

Fig. 3(c) was dictated by a lower E2 binding capacity of the NIP particles. According to our previous results, the MIP/NIP submicron particles scattered the excitation light (at 279 ± 1 nm) [19]. The fluorescence emission peaks (at 310 ± 1 nm) from E2–MIP to E2–NIP particles were slightly disturbed by the tail of this Mie scattering peak, but the fluorescence emission intensities after background subtraction were still valid for constructing Stern–Volmer plots (in Fig. 4). Two Raman scattering peaks were found at wavelengths around 380 and 425 nm; these light scattering peaks had no significant effects on the fluorescence emission intensities at 310 ± 1 nm.

Stern–Volmer (S–V) plots for fluorescence quenching usually exhibit a linear relationship between F_0/F and [Q] (see Eq. (1)). If the S–V plots show an upward-curving trend as evidenced by the date points in Fig. 4, the positive deviations from linearity represent a combined result from both static and dynamic (or collisional)

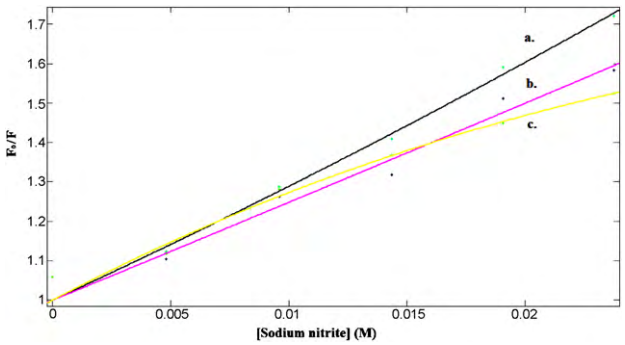

Fig. 4. Stern–Volmer plots of F_0/F versus concentration of sodium nitrite for (a) 4.5 ppm E2 aqueous solution, (b) 2.5 mg/mL E2–MIP particles in aqueous suspension and (c) 2.5 mg/mL E2–NIP particles in aqueous suspension. The solid lines indicate the best fittings from non-linear regression.

quenching [20]:

$$\frac{F_0}{F} = (1 + K_{SV}[Q])\ \exp^{(V[Q])} \quad (2)$$

where V is the static quenching constant.

The black line (a) is a non-linear regression curve for the S–V plot of 4.5 ppm E2 aqueous solution. The quenching constants were simulated with Matlab® (R2008b) to obtain $K_{sv} = 23.0 \pm 1.3\ M^{-1}$ and $V = 4.7 \pm 2.5\ M^{-1}$. The quenching constants for 2.5 mg/mL E2–MIP particles were $K_{sv} = 21.8 \pm 1.3\ M^{-1}$ and $V < 1.00\ M^{-1}$. For E2–NIP particles, $K_{sv} = 19.4 \pm 1.2\ M^{-1}$ and $V < 1.00\ M^{-1}$. The static quenching constant of E2 (without any particles) shows a higher value than those for E2–MIP and NIP particles. Apparently, the MIP/NIP particles disturbed the static quenching process. This may be attributed to the binding mechanisms between E2 and MIP/NIP particles. As proposed by Zhongbo and Hu, non-specific interaction (called surface binding) occurred between MIP particles and E2 molecules especially in water due to their hydrophobic nature, via hydrogen bonding [18]. The static quenching constant for E2 aqueous solution was larger than those for E2–MIP/NIP particles. This means the E2 molecules were protected inside the particles. Some functional groups of the E2 molecule were no longer available to interact with the quencher and form a non-fluorescent complex. The K_{sv} and V results for E2–MIP and E2–NIP particles were not very distinguishable due to the small size of nitrite anions. These small ions could easily infiltrate the porous MIP/NIP particles and quench the fluorescence of E2 molecules inside. Another disadvantage of using sodium nitrite as a quencher to investigate the porous structure of MIP particles by fluorescence quenching of E2 bound inside was that sodium nitrite exhibited a fluorescence emission peak (at 335 ± 1 nm) that interfered with the E2 fluorescence peak, especially at lower concentrations of E2 inside the particles.

Fig. 3(a) shows the fluorescence emission spectra of 4.5 ppm E2 aqueous solution progressively quenched by titration with sodium nitrite.

Unlike the ionic quencher (sodium nitrite), the molecular quencher methacrylamide has a larger size and more steric conformation. Fig. 5(a) shows the fluorescence emission spectra of 4.5 ppm E2 aqueous solution progressively quenched by titration with methacrylamide. After 0.07 M of methacrylamide was titrated into 3 mL of the E2 aqueous solution, approximately 86% of fluorescence emission from E2 was quenched. A broad fluorescence emission peak from methacrylamide was observed at 418 ± 3 nm (but of low intensity (even for 0.07 M). Fig. 5(b) and (c) shows the fluorescence quenching spectra of E2–MIP and E2–NIP particles, respectively. The increasing intensity at wavelengths below 300 nm was caused by Mie scattering (of the 279 ± 1 nm excitation light) from the particles. This Mie scattering peak did not cause any

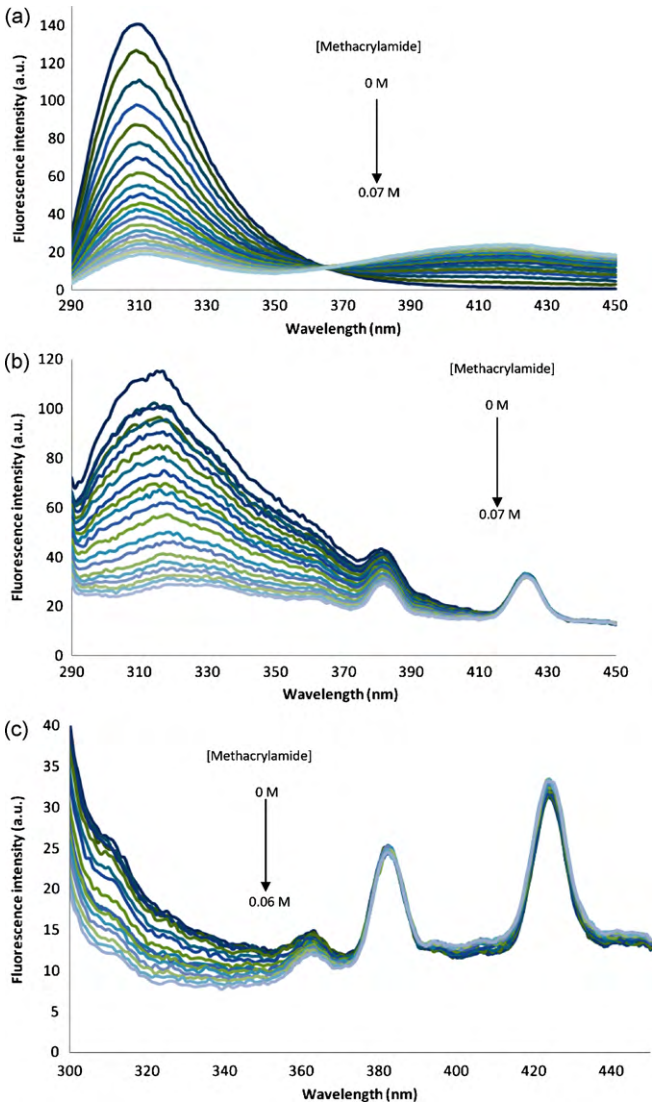

Fig. 5. Fluorescence emission spectra of (a) 4.5 ppm E2 aqueous solution, (b) 2.5 mg/mL E2–MIP particles in aqueous suspension and (c) 2.5 mg/mL E2–NIP particles in aqueous suspension, during titration with methacrylamide up to a final concentration of 0.07 M (without causing any significant dilution effects).

significant interference with the measurement of E2 fluorescence emission intensity in this study. Apparently, 76% of fluorescence emission from the E2–MIP particles (in aqueous suspension) was quenched by 0.07 M of methacrylamide, as well as 54% of fluorescence emission from the E2–NIP particles.

The S–V plots for fluorescence quenching by methacrylamide are shown in Fig. 6. Non-linear regression fitting, presented as solid lines through the data points had correlation coefficients as high as 0.9914. The dynamic and static quenching constants for 4.5 ppm E2 aqueous solution were 24.5 ± 2.4 and $4.0 \pm 1.0\ M^{-1}$, respectively. In comparison with sodium nitrite, methacrylamide exhibited quite similar dynamic and static quenching abilities. Both E2–MIP and E2–NIP particles exhibited very low dynamic quenching constants ($<1.00\ M^{-1}$ for both E2–MIP and E2–NIP) but strong static quenching constants ($V = 9.9 \pm 2.0\ M^{-1}$ for E2–MIP and $4.1 \pm 1.1\ M^{-1}$ for E2–NIP). One plausible explanation is that methacrylamide molecules are too large in size to be an effective dynamic quencher for collision with E2 molecules, bound inside the particles, under diffusion control. In this situation, static quenching became the dominant quenching mechanism for the E2. No sig-

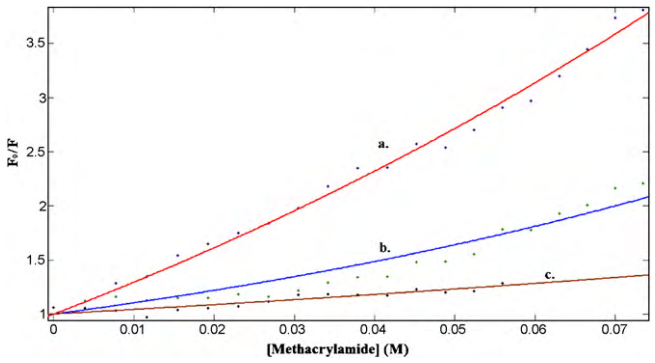

Fig. 6. Stern–Volmer plots of F_0/F versus concentration of methacrylamide for (a) 4.5 ppm E2 aqueous solution, (b) 2.5 mg/mL E2–MIP particles in aqueous suspension and (c) 2.5 mg/mL E2–NIP particles in aqueous suspension. The solid lines indicate the best fittings from non-linear regression.

nificant steric hindrance existed for methacrylamide molecules to infiltrate the porous structure of MIP/NIP particles.

The MIP particles had a porous structure consisting of imprinted cavities to selectively bind with E2 molecule. These cavities were unique in size, shape and functional groups that matched the 3-D molecular structure of E2. Other molecules would not be able to bind with the MIP, or to disrupt the E2–MIP binding of strong affinity. For quenching of the fluorescence emission from E2 (bound inside the imprinted cavities), methacrylamide might not suitable because it is sterically hindered in penetrating the imprinted cavities of MIP particles. However, the nitrite anions have a small size and planar 2-D structure, which facilitated their infiltration of MIP particles and get into the imprinted cavities with minimal resistance. This allowed the nitrite anions to penetrate the imprinted cavities and collide with the bound E2 molecules (which resulted in dynamical quenching of the fluorescence emission from E2 molecules). Contrarily, the methacrylamide molecules are too large to have this penetration capability for dynamically quenching the fluorescence emission from E2 inside the MIP cavities. The dynamic quenching constants of methacrylamide for E2–MIP particles (in aqueous suspension) were reasonably small ($K_{sv} < 1.0\,M^{-1}$). In fact, E2 aqueous solutions exhibited decreasing dynamic quenching constant values, with lower concentrations of E2 aqueous solution because the chance of collision between E2 molecules and quenchers would become smaller. Low E2 concentrations also caused decreasing static quenching constant values for both quenchers. The static quenching constant is based on the formation of 1:1 dark complex. When the concentration of E2 got lower, the rate of complex formation would be reduced and thus the static quenching constant values would decrease concomitantly. The static quenching constants for different concentrations of E2–MIP particles are interesting to examine. The quenching constant values for methacrylamide decreased with decreasing E2–MIP concentrations, which was the same with E2 aqueous solutions. For nitrite, the increasing static quenching constants with decreasing E2–MIP concentrations were caused by the artifact of fluorescence emission interference by the nitrite anion (around 335 nm). This presents a major disadvantage of using sodium nitrite in step (f) of the method described in Section 1, especially during the sensing of E2 at trace levels.

The NIP particles had similarly a porous structure like the MIP particles. A major difference was that, during the NIP preparation, E2 was not present as template molecules in the polymerization. Due to the absence of template molecules, the NIP particles lacked the 3-D imprinted cavities for selective binding with E2. However, the observed quenching constants for E2–NIP were remarkably different from those of E2 aqueous solution. The dynamic quenching constant for E2–NIP particles with sodium nitrite decreased its value from 19.4 to less than $1.0\,M^{-1}$ when the concentration of particles was reduced from 2.5 to 0.1 mg/mL. This also can be explained with the less opportunity to have collision between E2–NIP particles and nitrite ions. When methacrylamide was used to quench the fluorescence emission from E2–NIP particles, the dynamic quenching constant values were mostly less than $1.0\,M^{-1}$. This phenomenon may be explained by the interaction between the MAA-based NIP particles with methacrylamide due to similarity in molecular structure. Nonetheless, this interaction prevented collision between the bound E2 and methacrylamide.

4. Conclusions

Several interesting physico-chemical results were obtained from our experiments: (1) the particle sizes of MIP and NIP are 477 ± 11 and 373 ± 21 nm in diameter, respectively possibly as the result of adding E2 as a template in the former, (2) the fluorescence emission peaks of E2–MIP and E2–NIP are both found at $\lambda_{em} = 310 \pm 1$ when using $\lambda_{ex} = 280 \pm 1$ nm. No difference is observed between the excitation and emission spectra of E2–MIP and E2–NIP and (3) the non-linear fluorescence quenching model is properly elucidating the porous structure of MIP and NIP particles. The small 2-D planar nitrite ions penetrate the pores and quench the fluorescence emission from E2 inside by collision; a significant decrease of the dynamic quenching constant is obtained. Contrarily, the large 3-D stearic methacrylamide molecules are hindered in penetrating the pores, resulting in much smaller dynamic quenching constant values than those for the nitrite ion. Further research will be carried out in our laboratory to find a larger quencher molecule (than methacrylamide) to fulfill step (c) in the method described in Section 1. Metal nano-particles with a size hundreds of times larger than organic quenchers will be adopted in our further E2–MIP/E2–NIP fluorescence quenching research. For instance, Au nano-particles with a diameter ranging from 5 to 50 nm are an ideal large-size quencher for step (c) [21–23]. A better quencher ion (than nitrite) will also be needed for step (f) of the method, especially during the sensing of E2 at trace levels.

Nevertheless, methacrylamide is a functional monomer that has previously used to prepare MIP particles [24]. All methacrylamide-based MIP particles have a fluorescence quencher built in them. It can directly quench the fluorescence emission from any E2 molecules bound inside each particle. These particles can serve in the quick monitoring of E2 concentration in a water sample, by easily measuring the reduction of fluorescence emission from the sample (due to quenching) after E2 molecules bind with the particles with strong affinity and high selectivity. In our future work, an E2 biochemical sensor will be constructed of methacrylamide-based MIP. It can quickly determine the unknown E2 concentration in environmental water samples, or the E2 level in pre-menopausal woman's body fluids for her health care.

Acknowledgment

Financial support of the Natural Sciences and Engineering Research Council (NSERC) Canada is gratefully acknowledged.

References

[1] C.J. Allender, Molecularly imprinted polymers: technology and applications—preface, Adv. Drug Deliv. Rev. 57 (2005) 1731–1732.
[2] R. Rajkumar, M. Katterle, A. Warsinke, H. Moehwald, F.W. Scheller, Thermometric MIP sensor for fructosyl valine, Biosens. Bioelectron. 23 (2008) 1195–1199.
[3] K. Yano, I. Karube, Molecularly imprinted polymers for biosensor applications, Trac-Trends Anal. Chem. 18 (1999) 199–204.
[4] K. Uezu, H. Nakamura, J. Kanno, T. Sugo, M. Goto, F. Nakashio, Metal ion-imprinted polymer prepared by the combination of surface template polymerization with postirradiation by gamma-rays, Macromolecules 30 (1997) 3888–3891.

[5] N. Gao, Z. Xu, F. Wang, S.J. Dong, Sensitive biomimetic sensor based on molecular imprinting at functionalized indium tin oxide electrodes, Electroanalysis 19 (2007) 1655–1660.
[6] L. Schweitz, L.I. Andersson, S. Nilsson, Rapid electrochromatographic enantiomer separations on short molecularly imprinted polymer monoliths, Anal. Chim. Acta 435 (2001) 43–47.
[7] E. Caro, R.M. Marce, F. Borrull, P.A.G. Cormack, D.C. Sherrington, Application of molecularly imprinted polymers to solid-phase extraction of compounds from environmental and biological samples, Trac-Trends Anal. Chem. 25 (2006) 143–154.
[8] C.R. Stockard, G.N. Papanicolaou, The existence of a typical oestrous cycle in the guinea-pig - with a study of its histological and physiological changes, Am. J. of Anat. 22 (1917) 225–283.
[9] E. Allen, A.E. Doisy, An ovarian hormone: preliminary report on its localization, extraction, and partial purification and actions in test animals, J. Am. Med. Assoc. 81 (1923) 819–821.
[10] M. Luconi, G. Forti, E. Baldi, Genomic and nongenomic effects of estrogens: molecular mechanisms of action and clinical implications for male reproduction, J. Steroid Biochem. Mol. Biol. 80 (2002) 369–381.
[11] N.B. Ojeda, D. Grigore, E.B. Robertson, B.T. Alexander, Estrogen protects against increased blood pressure in postpubertal female growth restricted offspring, Hypertension 50 (2007) 679–685.
[12] B. Brunstrom, J. Axelsson, A. Mattsson, K. Halldin, Effects of estrogens on sex differentiation in Japanese quail and chicken, Gen. Comp. Endocrinol. 163 (2009) 97–103.
[13] G.J. Pepe, E.D. Albrecht, Actions of placental and fetal adrenal steroid hormones in primate pregnancy, Endocrinol. Rev. 16 (1995) 608–648.
[14] E.D. Albrecht, G.W. Aberdeen, G.J. Pepe, The role of estrogen in the maintenance of primate pregnancy, Am. J. Obstet. Gynecol. 182 (2000) 432–438.
[15] R.J. Golden, K.L. Noller, L. Titus-Ernstoff, R.H. Kaufman, R. Mittendorf, R. Stillman, E.A. Reese, Environmental endocrine modulators and human health: an assessment of the biological evidence, Crit. Rev. Toxicol. 28 (1998) 109–227.
[16] S. Wei, A. Molinelli, B. Mizaikoff, Molecularly imprinted micro and nanospheres for the selective recognition of 17beta-estradiol, Biosens. Bioelectron. 21 (2006) 1943–1951.
[17] R.A. Leese, E.L. Wehry, Corrections for inner-filter effects in fluorescence quenching measurements via right-angle and front-surface illumination, Anal. Chem. 50 (1978) 1193–1197.
[18] Z. Zhongbo, J. Hu, Selective removal of estrogenic compounds by molecular imprinted polymer (MIP), Water Res. 42 (2008) 4101–4108.
[19] Y. Yang, E.P.C. Lai, M. Liu, Spectroscopic analysis of poly(methacrylic acid-co-ethylene glycol dimethacrylate) submicron particles by fluorescence emission and light scattering upon binding with 17β-estradiol in water treatment, Open Colloid Sci. J. 3 (2010) 1–8.
[20] J.R. Lakowicz, Principles of Fluorescence Spectroscopy, 3rd ed., Springer, 2006.
[21] J. Zhang, R. Badugu, J.R. Lakowicz, Fluorescence quenching of CdTe nanocrystals by bound gold nanoparticles in aqueous solution, Plasmonics 3 (2008) 3–11.
[22] S.Y. Lim, J.H. Kim, J.S. Lee, C.B. Park, Gold nanoparticle enlargement coupled with fluorescence quenching for highly sensitive detection of analytes, Langmuir 25 (2009) 13302–13305.
[23] S. Mayilo, M.A. Kloster, M. Wunderlich, A. Lutich, T.A. Klar, A. Nichtl, K.K. rzinger, F.D. Stefani, J. Feldmann, Long-range fluorescence quenching by gold nanoparticles in a sandwich immunoassay for cardiac troponin T, Nano lett. 9 (2009) 4558–4563.
[24] V. Pichon, F. Chapuis-Hugon, Role of molecularly imprinted polymers for selective determination of environmental pollutants—a review, Anal. Chim. Acta 622 (2008) 48–61.